PROCEEDINGS OF SCIENCE

Neutron Monitor as a Calorimeter to Measure Particle Spectra

Paul Evenson,[a,*] **John Clem,**[a] **Pierre-Simon Mangeard,**[a] **Waraporn Nuntiyakul,**[b] **David Ruffolo,**[c] **Alejandro Saiz,**[c] **Achara Seripienlert,**[d] **Surujhdeo Seunarine**[e] **and Chanoknan Banglieng**[f]

[a] *University of Delaware, Physics and Astronomy*
Newark, DE 19716 USA
[b] *Chiang Mai University*
Chiang Mai, Thailand
[c] *Mahidol University*
Bangkok, Thailand
[d] *National Astronomical Research Institute of Thailand (NARIT)*
Chiang Mai 50180, Thailand
[e] *University of Wisconsin River Falls*
River Falls, WI, USA
[f] *Rajamangala University of Technology Thanyaburi*
Pathum Thani, Thailand

E-mail: evenson@udel.edu, jmc@udel.edu, s.author@univ.country

Magnetic activity on the sun influences the flux of galactic cosmic rays at Earth in the process known as solar modulation. While most pronounced at 1 GeV and below, it also operates at much higher energy, still exhibiting solar magnetic polarity dependence. Historically, an observational gap exists between approximately 17 GeV (the highest geomagnetic cutoff) neutron monitor data and muon observations of primary cosmic rays that are mostly above 50 GeV. We have shown that a neutron monitor can be used as a calorimeter to measure the spectrum of atmospheric secondaries, and thus to infer the primary spectrum. In this paper we examine data over an extended time interval to explore the need to correct for barometric pressure. We compare the results of the calorimeter method to other local measures of the particle spectrum, such as the leader fraction.

38th International Cosmic Ray Conference (ICRC2023)
26 July - 3 August, 2023
Nagoya, Japan

∗Speaker

PoS(ICRC2023)1233

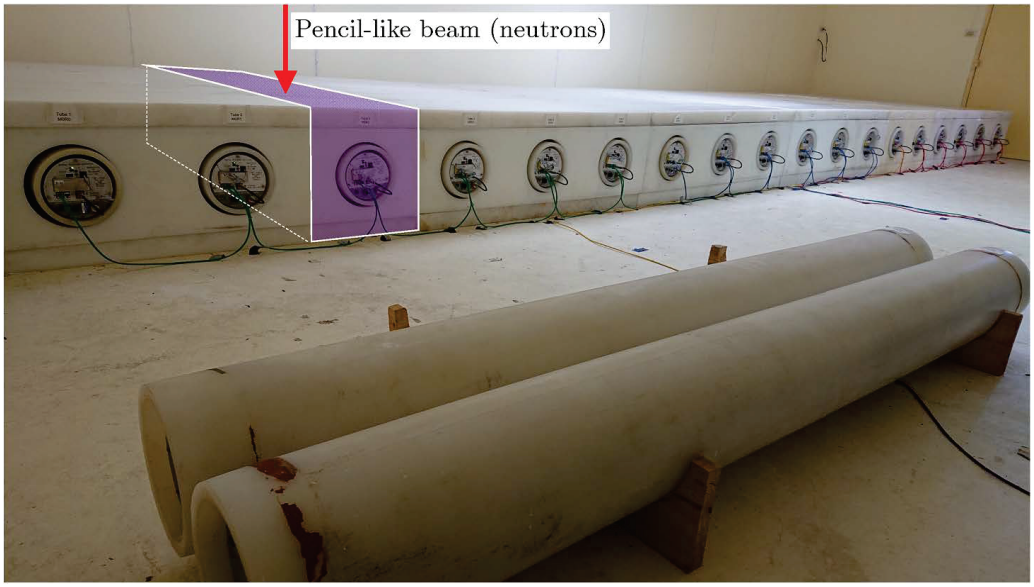

Figure 1: Annotated photograph of the Princess Sirindhorn Neutron Monitor (PSNM), indicating a simulated pencil-like beam of neutrons.

1. Introduction

Detecting multiple neutrons from the same primary particle has long been discussed as a means to estimate the primary energy spectrum from a single neutron monitor [1]. The first definitive use was outlined in [2]. Over the past few years we have used details of the timing distribution of individual neutron detections to show that the shape of the cosmic ray spectrum at approximately 17 GV is still being influenced by solar magnetic polarity [3]. Beginning in 2015 we upgraded the electronics at PSNM to record pairwise correlations among detectors to improve the energy resolution of this technique [4, 5]. We have shown that detecting and categorizing multiple interactions allows estimation of the spectrum of secondary particles striking the monitor [6]. In this paper we examine data over an extended time interval to explore corrections for barometric pressure.

2. Technical Details

Figure 1 shows a photograph of PSNM, with 18 NM64 *units* enclosed in a polyethylene housing, generally called the *reflector*. Each unit consists of a boron trifluoride proportional counter enclosed in a lead *producer* and polyethylene *moderator*. Additional moderated boron trifluoride counters, located outside the reflector, are referred to as *bares*.

We define further terminology: Cosmic rays incident on the atmosphere are referred to as *primary* particles. The products of interaction in the atmosphere are termed *secondary* particles, while a particle entering the monitor itself is called an *incident* particle. Thus, in the photo, a pencil beam of incident neutrons illuminates unit 2. Signals recorded in the units (most commonly a single neutron) are referred to as *hits*. Each hit is time-tagged and related to GPS time to an accuracy of 2 microseconds. Groups of hits are referred to as *events*, and events satisfying certain criteria are referred to as *catches*.

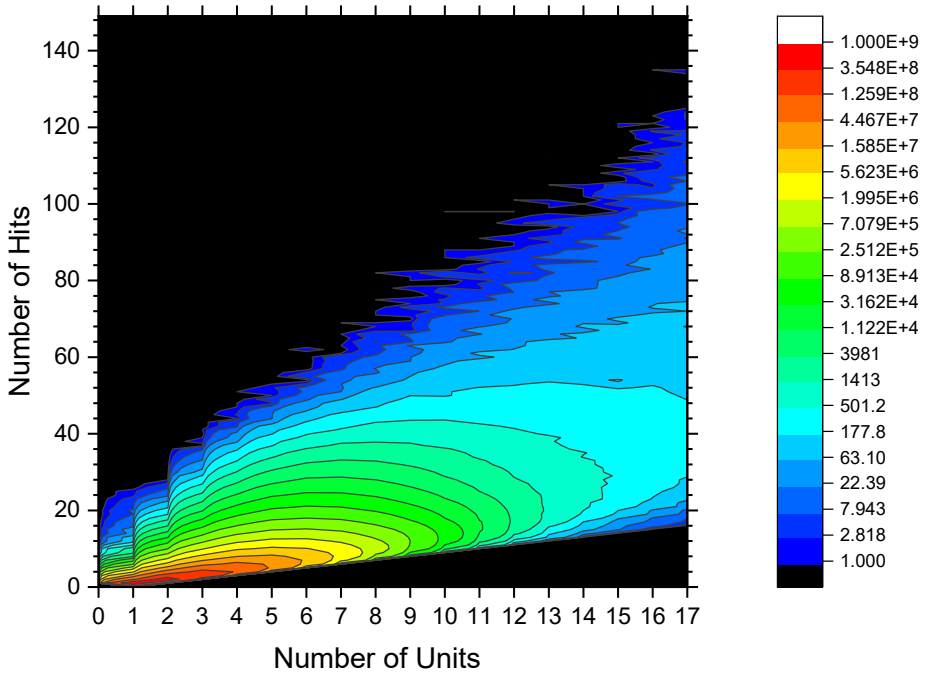

Figure 2: Catches Recorded at PSNM

All hits are made available in real time to the software in the data acquisition system (DAQ). The hit rate in the NM64 units is about 34 Hz, while the bares operate at about 6 Hz. The DAQ generates histograms of time delays between successive hits in individual units, as well as pairwise delays in 54 different classes of unit pairs (nearest neighbors, second nearest, etc.) More complex situations are recorded individually as catches, which form the basis for the analysis in this paper. Typically the only outputs are the histograms (hourly) and the catches, but it is possible to record all hits (the so-called *HitSpool*) for offline development of catch criteria.

Operation of the DAQ is illustrated in Figure 2 via a matrix displayed as a contour plot. The number of units in a catch is shown horizontally while the total number of hits, summed over all units, forms the vertical dimension. The structure in the lower left part of the matrix results from the finite deadtime (approximately 90 microseconds) of the DAQ. Most of the neutrons are detected within 2 milliseconds of the initial interaction so a single unit typically cannot record more than about 10 hits in a catch.

The larger catches are almost entirely due to close air shower cores. Our primary concern at this time is identification of interactions that result from primaries in the energy range relevant to modulation. In doing this we are being guided by the results of simulations using FLUKA [9, 10] discussed in some detail in [6]. Incident particles in the energy range one to a few hundred GeV produce quite characteristic signals in the monitor, very unlike the signals from air shower cores. The unit most directly in the path of the entering particle has the largest number of hits, while the neutrons spread out in smaller numbers at later times to the adjacent units. This is consistent with

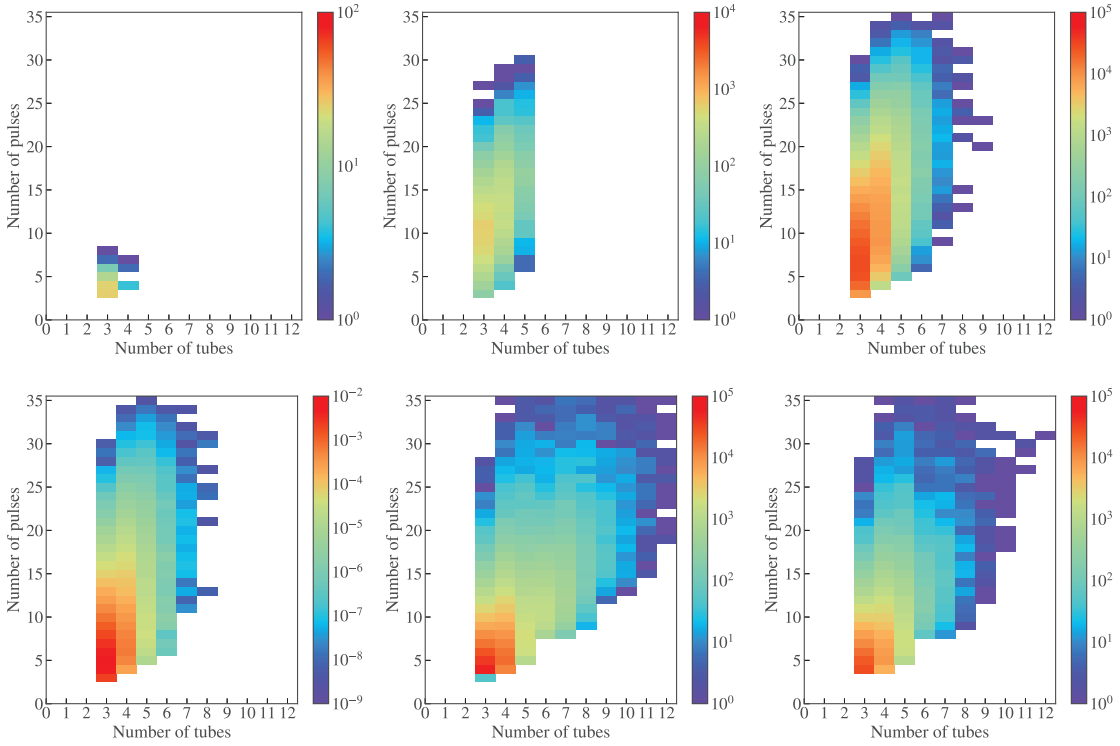

Figure 3: Response of PSNM to incident particles. Top left two panels: Simulated 1 and 100 GeV, pencil beam, normal incidence. Top right: Simulated 1 to 100 GeV $E^{-1.0}$ spectrum, uniform illumination at variable zenith angles. Bottom left: The 1 to 100 GeV spectrum re-weighted to $E^{-2.5}$. Bottom center: Approximately two days of data from PSNM. Bottom right: Compact (as defined in the text) subset of actual data.

a diffusion-absorption picture of the neutron propagation [11].The maximum number of hits from incident particles increases nearly linearly with particle energy. Unfortunately, high energy incident particles produce many events that are indistinguishable from those initiated by lower energy particles. Figure 3 has the same general format as Figure 2. The upper left panel is for a 1 GeV (monoenergetic) pencil beam incident as in Figure 1 and the upper center is for 100 GeV. The upper right panel shows a simulation of an $E^{-1.0}$ spectrum of neutrons from 1 to 100 GeV, distributed over the monitor with incident angles from 0 to 45 degrees. The lower left panel shows the same simulation weighted as an $E^{-2.5}$ spectrum. The lower center panel shows approximately two days of data taken at PSNM using the catch criterion (3/3: three or more units, three or more total hits).

A simple analysis, constructed from the columns in the lower right panel of Figure 3, is shown in Figure 4. In the upper left panel the column of total hits for exactly three units hit is displayed as a histogram, with the data as the red points. The histogram is truncated at seven total hits because the simulation (at this time) has only been done between 1 and 100 GeV. Guided by Figure 3 incident particles below 1 GeV will contribute minimally to this histogram. The weighting of the simulated data is then adjusted as a power law to produce the best fit (minimum chi-square) indicated by the blue line. We can also compute the mean position of the hit cluster from data and simulation as shown in the top center panel. In both cases the data follow the simulation within errors.

The expected spectrum of incident particles calculated by the EXPACS 410 program [12–14]

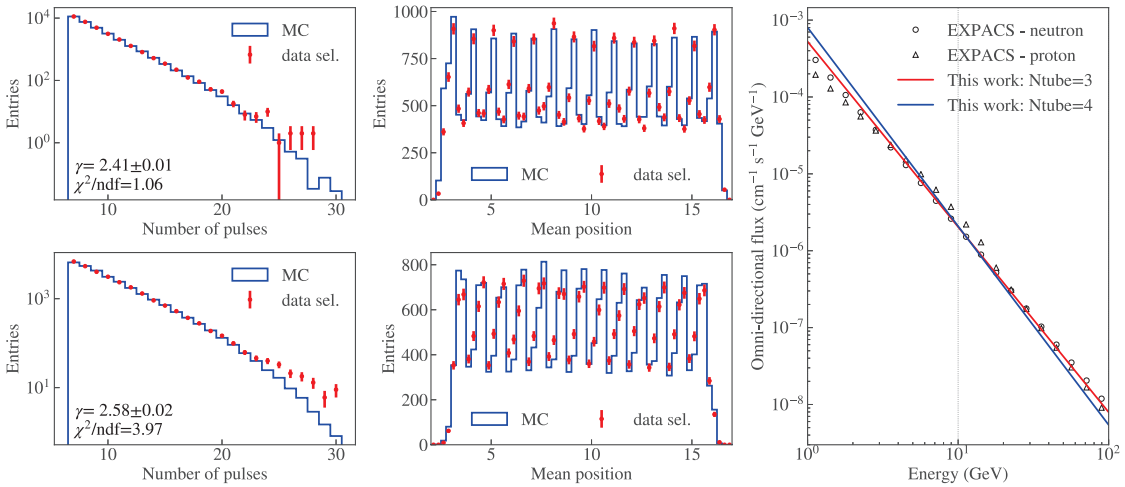

Figure 4: Results of fitting compact data further restricted as discussed in the text.

for the time and location of the data is shown in the right panel of Figure 4 as black symbols. EXPACS calculates both protons and neutrons, whereas our simulation to date only considers neutrons. The best fit spectra from the left panels (arbitrarily normalized at 10 GeV) are shown as red (for 3 units) and blue (for 4 units) lines. For such a simple analysis we find the agreement remarkable, with some indication of better agreement for the case assumed to have less background.

3. Barometer Corrections

With a view to observing long term trends in the particle spectrum we have begun to focus on possible corrections due to environmental variations, beginning with the barometric pressure. One might imagine several approaches to correcting a spectrum like that in Figure 4. The one we are presently investigating is based on the traditional neutron monitor practice of correcting a count rate using a barometric coefficient ($C_p = C\exp[\beta(p - p_{\rm ref})]$) determined empirically from the data. In turn, each "cell" in the matrix shown in Figure 2 is simply a count rate reflecting an individual yield function convoluted with the primary spectrum. Properly understood the yield functions include the "migration" of counts from one cell to another. We can then assume that each cell also has a specific barometer coefficient that can be determined by examining the correlation between variations in count rate and barometer reading. Figure 5 illustrates the statistically significant barometer coefficients that we have been able to extract from data running from April through June of 2023. Some overall systematics are present but the statistical accuracy for many "cells" is still marginal. Note that some of the coefficients are positive – the cells gain counts with increased pressure as the "inflow" exceeds the "outflow". In our further analysis we use the fit lines shown to define and extrapolate the coefficients to regions where the direct determination is not statistically useful.

To examine time evolution we consider "compact" events defined as consisting of a contiguous group of three or four units, not including an end unit, with no other hits in the monitor. We further construct a simple spectrum consisting or three "bands". The low band has from 4 to 9 total hits, the middle band 10 to 14 and the high band 15 or more total hits. Figure 6 shows daily averages of

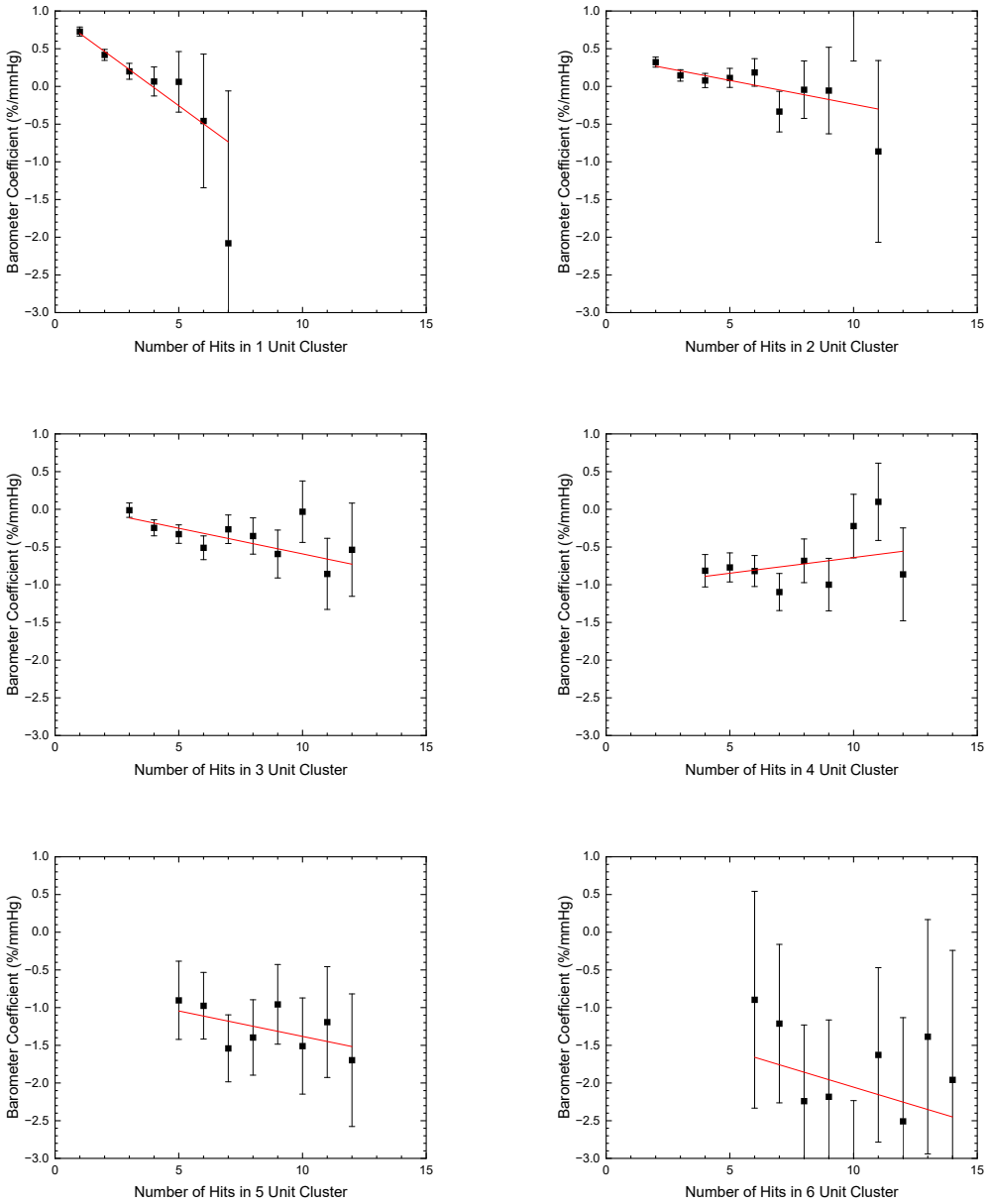

Figure 5: Barometer Coefficients

one hour count rates for the full PSNM monitor and the low band of compact catches. The overall time structure is similar but not identical.

4. Results and Conclusions

The left panel of Figure 7 compares the two rates directly as a scatterplot, which exhibits the overall common trend but has deviations considerably greater than the assigned statistical errors. Points in red indicate days that have been arbitrarily excluded from all analysis due to their large

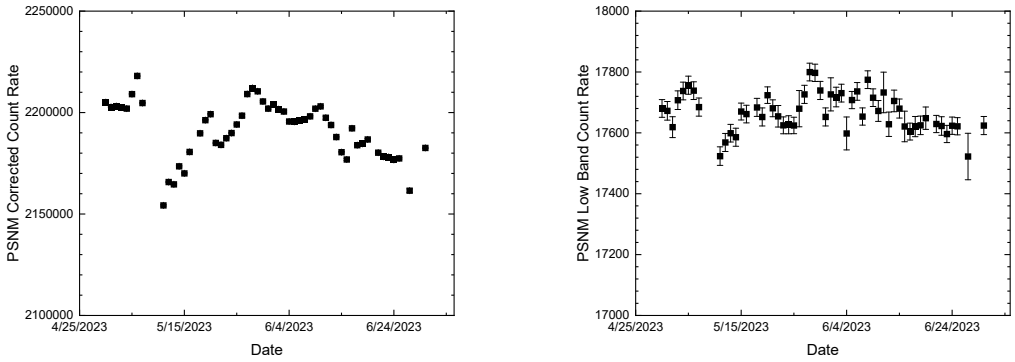

Figure 6: Daily average count rates (events per hour) as a function of time. Left: Pressure corrected total counts. Right: Low band as described in the text.

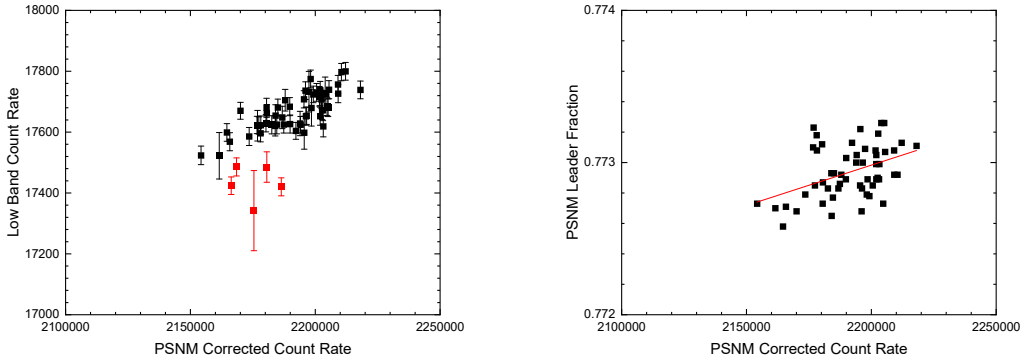

Figure 7: Daily averages comparing low band catches and leader fraction to total count rate. Left: Low band – red points excluded as noted in text. Right: Leader fraction.

deviations. The full reason for the deviations is not clear at this point, but all the days involved have data gaps of one kind or another. Note the highly suppressed zero of the scale – these are tiny fluctuations that are hard to relate to specific events in the data. Plots for the middle and high bands are not displayed as they show no statistically significant time dependence. At present we take this primarily to indicate that our pressure corrections are reasonable and these bands do reflect higher energy particles that are less affected by modulation in the solar wind.

The right panel shows the leader fraction [3] as a similar scatterplot. The leader fraction is known to reflect changes in the cosmic ray spectrum near the geomagnetic cutoff of the neutron monitor. Coupled with the constancy of the higher bands it is likely that changes in the spectrum of catches indeed reflect variations of the primary cosmic ray spectrum.

At this point it is difficult to make more precise statements. We need both simulations and better statistics to assign particle energy ranges to the bands and to refine the definition of the bands. While we work towards this we will continue to take data at PSNM with the objective of tracking the evolution of the spectrum through the present solar maximum and upcoming magnetic polarity

reversal.

This work was supported in part by United States National Science Foundation Simpson award, NSF2112439, the National Science and Technology Development Agency (NSTDA) and the National Research Council of Thailand (NRCT) under the High-Potential Research Team Grant Program (N42A650868), NRCT (N42A661044), and NSRF via the Program Management unit for Human Resources & Institutional Development, Research and Innovation (B37G660015).

References

[1] Dyring, E. & B. Sporre, Latitude effect of neutron multiplicity as detected by a shipborne neutron monitor, *Ark. Geofys.* **5**, 67, 1966

[2] Ruffolo, D., *et al.*, Monitoring short-term cosmic-ray spectral variations using neutron monitor time-delay measurements, *ApJ* **817**, 38, 2016

[3] Banglieng, C., *et al.*, Tracking Cosmic-Ray Spectral Variation during 2007–2018 Using Neutron Monitor Time-delay Measurements, *Astrophys. J.* **890**, 21, 2020

[4] Sáiz, A., *et al.*, Measurement of cross-counter leader fractions in an 18NM64: Detecting single and multiple atmospheric secondaries, *Proc. 35th ICRC (Busan)* PoS(ICRC2017)047, 2017

[5] Sáiz, A., *et al.*, Detecting single and multiple atmospheric secondaries in an 18NM64, *Proc. 36th ICRC (Madison)* PoS(ICRC2019)1145, 2019

[6] Evenson, P., *et al.*, Multiple Particle Detection in a Neutron Monitor, *Proc. 37th ICRC (Berlin)* PoS(ICRC2021)1240, 2021

[7] Antoni, T., *et al.*, Electron, muon, and hadron lateral distributions measured in air showers by the KASCADE experiment, *Astroparticle Physics* **14**, 245-260, 2001

[8] Antoni, T., *et al.*, The cosmic-ray experiment KASCADE, *NIM A* **513**, 490 – 510, 2003

[9] Battistoni, *et al.*, Overview of the FLUKA code, *Annals of Nuclear Energy* **82**, 10-18, 2015.

[10] Bohlen, T.T., *et al.*, The FLUKA Code: Developments and Challenges for High Energy and Medical Applications, *Nuclear Data Sheets* **120**, 211-214, 2014

[11] Chaiwongkhot K., *et al.*, Measurement and simulation of the neutron propagation time distribution inside a neutron monitor, *Astroparticle Physics* **132**, 102617, 2021

[12] Sato, T., Analytical model for estimating terrestrial cosmic ray fluxes nearly anytime and anywhere in the world: Extension of PARMA/EXPACS, *PLOS ONE* **10(12)** e0144679, 2015

[13] Sato, T., Analytical Model for Estimating the Zenith Angle Dependence of Terrestrial Cosmic Ray Fluxes, *PLOS ONE***11(8)** e0160390, 2016

[14] https://phits.jaea.go.jp/expacs/